World Journal of Engineering Research and Technology
WJERT
www.wjert.org
SJIF Impact Factor: 5.924

A STUDY OF DC-DC CONVERTERS DYNAMIC MODES USING ENERGY FUNCTIONS

Yefim Berkovich* and Sagi Moshe

Department of Electrical Engineering, Holon Institute of Technology, 52 Golomb st., Holon, 58102, Israel.

Article Received on 05/05/2021 **Article Revised on 26/05/2021** **Article Accepted on 16/06/2021**

***Corresponding Author**
Yefim Berkovich
Department of Electrical Engineering, Holon Institute of Technology, 52 Golomb st., Holon, 58102, Israel.

ABSTRACT

The present paper is a study of dynamic modes in DC-DC converters on the basis of energy principles. As is known, the dynamic modes in converters are usually analyzed by forming differential equations systems according to Kirchhoff's laws – also using commutation functions – and subsequently solving them. This leads to non-linear equations of high orders, solved by the averaging method and that by small signal analysis. The analysis turns out to be work consuming and its results are cumbersome and non-transparent, so in practice they can be only applied to the simplest converters. At the same time, with the progress in power electronics the converters' designs are becoming considerably more complicated, making it relevant to seek others, more efficient methods of study. In the present paper the analysis of converter dynamics is based on an approach, which long ago has become classical in mechanics and other fields, yet is still rarely used in electrical engineering. It is based on the use of a function containing the values of the magnetic and electrical energy in a circuit, that is, the function called the Lagrangian which makes it possible to rather easily obtain linearized equations for the averaged voltages and currents values, as well as corresponding linear circuits, the dynamic processes in which are identical with those going on in original converters. In order to illustrate the opportunities and efficiency of the approach, we have made an analysis of the dynamics of all the base converters: the buck-, boost- and buck-boost converters, as well as the Cuk, Sepik and Zeta converters. We also have analyzed a number of converters with more complex structures

having an increased number of reactive elements, which more clearly exemplify the advantages of the present approach. All our theoretical results have been confirmed by computer experiments and, in addition, many of the converters under consideration were realized as laboratory models and tested experimentally. The results of the experiments completely confirm our theoretical conclusions.

KEYWORDS: DC-DC Converters, Dynamic Modes, Energy Functions, Lagrangian, Hamiltonian, Linearization.

I. INTRODUCTION

The analysis of the dynamic modes in DC-DC converters occupies an important place in their designing, allowing to identify in transient states possible excesses of the voltages and currents, to determine the durations of non-stationary modes, and, most important, to consider the converter as a link in an automatic control system. At present, such analyses are based on the groundbreaking work (Middlebrook, et al., 1976), which assumed the formation of differential equations systems based of Kirchhof's laws, their adjustment using the commutation functions, transitions to smooth components by averaging, and subsequently, their solutions for small increments by the Laplace transform. The approach given in (Middlebrook, et al., 1976) is a completely universal one, but even for the circuits of the second order it becomes cumbersome and non-transparent. Examples of the analysis of various types of converters are given in vast literature, in particular, in (Tripathi, et al., 2019, Vratislav, et al., 2016, Hayes, 2016, Axelrod, 2015).

While in the quoted approach, the continuous smooth components of the quantities are being selected, in another, also widespread approach, a lattice function of these quantities is taken, and the perturbations are written as δ-functions with subsequent solutions of the equations thus obtained by the z-transform (Axelrod, et al., 2005, Bahravar, et al., 2012).

It should be noted that in the last decades computer modeling is widely used for the study of converter dynamics (Hsu, et al., 1979, Agrawal, et al., 2014). It allows one to avoid many assumptions and simplifications which are inevitable in the above approaches based on linearization, averaging, or selection of lattice functions. This is especially valuable in the cases when the linearization of a system is inadmissible in principle, and it is necessary to preserve the non-linear character of the processes, in particular in the study of chaotic modes (Tse, 2004, Beck, et al., 2020, 2019, Zhioua, et al., 2014). However, for all its great

opportunities, the computer modeling remains an efficient, but an experimental approach. It suits less for establishing general patterns and relations, which is possible in the analytical approaches mentioned above.

At the same time, as early as in the 18-19 centuries in the analysis of dynamic modes in mechanics, basing on Newton's laws, on the works by J.R d'Alembert, J.L. Lagrange, L. Euler, W.R. Hamilton and other outstanding mathematicians, the important optimization principles were developed, which made it possible to determine the trajectories of motion of the most various nature: in mechanics, thermodynamics, quantum electrodynamics, electrical engineering (Gantmakher, 2005, Prigogine, et al., 1994, Simonyi, 1956, Wells, 1938). These principles are not only a reflection of the deep unity of nature's laws, but also they give new opportunities in the dynamic analysis modes of the very different nature phenomena. And they turn out to be very useful in the devises of power electronics, as will be illustrated in this paper on many examples.

As noted in (Dennis, 1959), as early as 1873, J.C. Maxwell determined optimization principles in electrical engineering noting that in electrical circuits that contain voltage or current sources and resistors, the distribution of currents that lead to minimal release of active power abides by Kirchhoff's laws. Maxwell's observation thus set another approach to the investigation of electrical circuits: when determining currents one should base not on Kirchhoff's laws, but on the condition of minimization of the released active power. This feature of electrical circuits has been used in many works for modeling the principles of minimizing the production of entropy as formulated by I. Prigogine, or its maximization, according to L. Onsager (Dennis, 1959, Martyushev, 2006, Landauer, 1975, Axelrod, et al., 2005).

It should be noted that despite the fact that in a more general case the optimization features of dynamic systems, including, of course, those in electrical engineering were formulated at least as early as in the 19th century, they, however, did not find their serious implementation in electrical engineering. Nevertheless, a number of publications did appear, which dealt with various aspects of electrical circuits on the basis of Hamilton's principle, Lagrange's energy functions (Hamiltonians, Lagrangians), and respective canonical equations.

As one of the first works in that direction, we may point out (Wells, 1938), which gives a short introduction into the formulation of the canonical equations of the Lagrangian and

quotes some examples of its use in the analysis of electrical circuits. In (Russer, et al., 2012), the application of Lagrange and Hamilton methods to classical electrical circuits and to circuit quantum electrodynamics circuits is presented. There is also a discussion on the formulation of the Lagrangian and Hamiltonian equations for lossless electrical circuits including linear and nonlinear circuit elements. Three examples of the application of optimization principles are given in (Mayer, 2001): a conservative electrical circuit with five capacitors basing on a Hamiltonian, and – using a Lagrangian – a non-conservative electrical circuit of the fourth order with two resistors, as well as an electromagnetic circuit, an electromagnetic actuator. In (Kadhim, 2016) the author studies different electrical circuits using the Lagrangian formalism: the LC-circuit, RL-circuit, coupled circuits and a simple example of a DC-DC power converter. In (Scherpen, et al., 1999, 2003, Yildiz, et al., 2009, Sira-Ramirez, et al., 1996) optimization methods based on a Lagrangian are used for analyzing various DC-DC power converters; this approach yielded Kirchhoff's equations, which nevertheless contained a commutation function, and which were later solved with the use of averaging the quantities in the equations. In (Skandarnezhad, et al., 2016), we see the same approach to analyzing DC-DC converters. A number of works illustrate the efficiency of the application of the Lagrangian for analyzing electrical circuits, including the converters with magnetic elements, in particular, three-phase transformers, (Lee, 2004, Tan, et al., 2008, Dworakowski, et al., 2020, Noah, et al., 2017, Umetani, 2015). One should also note a number of interesting publications on the use of the Lagrangian in power electronics, published in a collection (Umetani, 2015). The collection's seven sections analyze – with the use of the Lagrangian – the stationary modes of various converters, including their complex modifications with ZVS and ZCS, as well as those with complex magnetic systems. The collection's conclusion notes that our knowledge on the applications of Lagrangian dynamics to power electronics is scarce, although Lagrangian dynamics is widely applied in the mechanics areas. A particular attention should be given to a solid book on the application of optimization methods, (White, et al., 1959), devoted to electromechanical systems, and to (Soudakov, 2014), which gives examples of using the optimization approach to the linear purely conservative systems.

The present paper uses the optimization approach to analyzing dynamic modes in DC-DC converters of most various types and shows its essential advantages over those used now. The paper's composition is as follows. Section II is a brief introduction into the technique of the dynamics system's analysis using the optimization method, and Section III gives examples of

such analysis for the classic types of converters: boost-, buck-boost and buck converters. The next Section IV considers more complex fourth order converter circuits: Cuk-, Sepic and Zeta converters, while Section V consider widely used converters, which contain additional elements insuring increasing the transform coefficient of the output voltage. The theoretical results are being confirmed by computer modeling, and for some circuits, by experiments on a physical model, which also confirms the efficiency of the method proposed.

II. A brief introduction into the methods of analysis of dynamics system. Hamilton's principle and Lagrange's energy function

As is well known, and as we emphasized above, the finding of voltages and currents in dynamic modes of electrical appliances and systems is based on the solution of Kirchhoff's equations written in the form of differential equations. In that case, one could say that the finding of the unknown quantities is related to infinitely small changes in a system. At the same time, there is another approach to the dynamics study of various natures systems. It is based on the assertion that the sought quantities which form the trajectory of motion lead to optimization (more often, minimization) of an energy function of a system. In that case, the dynamic trajectory of a system is determined by the finding of an extremum of some integral functions by the methods of variational calculus, that is, with the principles connected, as was noted in (White, 1959), with a large-scale motion of a system. A physical system has the unique trajectory of motion independently of its description principle.

Hamilton's principle is considered to be the most fundamental integral principle of description. For its realization *N* independent coordinates of a system, $q_j(t)$, and the same number of the coordinates $\dot{q}_j(t)$ are introduced. In a mechanical system they are respectively the spatial coordinate and its momentum, in an electrical engineering system, they are the electrical charge and flux linkage. Note in advance that depending on the problem, the roles of these two quantities may replace one another. The common formulation of Hamilton's principle is that the variation of the time integral of a energy function $\mathcal{L}$ between two points, $q_j(t_1)$ and $q_j(t_2)$ should equal zero. We begin with defining a function *I* as the integral of an energy function $\mathcal{L}$.

$$I = \int_{t_1}^{t_2} \mathcal{L}(q_1,...,q_N;\dot{q}_1,...,\dot{q}_N;t)dt \qquad (1)$$

One of the formulations of Hamilton's principle is: the actual dynamic trajectory of the system described by the energy function $\mathcal{L}$, is determined by finding an extremum (usually, minimum) of the function *I*. This means that the independent of time variation δ of the function *I* must equal zero.

$$\delta I = \delta \int_{t_1}^{t_2} \mathcal{L}(q_1,...,q_N;\dot{q}_1,...,\dot{q}_N;t)dt = 0 \qquad (2)$$

and must obey the boundary conditions:

$\delta q_j(t_1) = 0$ and $\delta q_j(t_2) = 0$ for $j = 1,2,3,...,N.$

Now, it must be emphasized that the search of an extremum according to(2) results in determining a number of relations in the form of differential equations with respect to the coordinates q_j and their derivatives $\dot{q}_j$, satisfying.(2)

As the energy function, we choose the Lagrange function, the Lagrangian, whose great advantage is that it is suitable both for conservative and non-conservative systems. Moreover, it is important that, in the case of a non-conservative system, Lagrange's function can be applied only to its conservative part, and the influence of the non-conservative elements can be taken into account separately. This fact simplifies greatly the solving of the problem, since when considering converters, we consider first the part of the circuit consisting only of its reactive elements – inductors and capacitors – and later take into account the influence of the input voltages and resistors.

For a conservative system, Lagrange's function is the difference between the kinetic, $W_{\dot{q}}$, and potential, W_q, energies of the entire system.

$$\mathcal{L} = W_{\dot{q}} - W_q \qquad (3)$$

For a mechanical system, obviously, $W_{\dot{q}} = \sum_{j=1}^{N} \frac{\dot{q}_j^2}{2m_j} = \sum_{j=1}^{N} \frac{m_j v_j^2}{2}$, where m_j and v_j are the mass and velocity of the variation of the coordinate q_j respectively, while $W_q = \sum_{j=1}^{N} \frac{q_j^2}{2k_j} = \sum_{j=1}^{N} \frac{k_j q_j^2}{2}$, where k_j it is some coefficient, for example, the stiffness of a spring. For an electrical engineering system, when one choses the flux linkages $L_j i_j$ as the coordinates q_j, and the

charge of the capacitors $C_j v_j$ as the coordinates $\dot{q}_j$, they are respectively the energy of the electric and magnetic fields:

$$W_{\dot{q}} = \sum_{j=1}^{N} \frac{(C_j v_j)^2}{2C_j} = \sum_{j=1}^{N} \frac{C_j v_j^2}{2} \tag{4}$$

and

$$W_q = \sum_{j=1}^{N} \frac{(L_j i_j)^2}{2L_j} = \sum_{j=1}^{N} \frac{L_j i_j^2}{2} \tag{5}$$

Here and hereafter L_j and i_j are respectively the inductance and the current through it, C_j and v_j are respectively the capacitance and voltage on it. It is necessary to emphasize that in order for the energy $W_{\dot{q}}$ to be the energy of the coordinate $\dot{q}_j$, the charges of the capacitances were of the form of the derivatives of the flux linkages. When one chooses, on the contrary, as the coordinate q_j, the charge of the capacitors $C_j v_j$ and, as the coordinate $\dot{q}_j$ of the flux linkages $L_j i_j$, the latter should be written as the derivatives of charges.

Basing on the concrete form of the energy function (3), using the solution of the integral equation (2), we find a system of *N* differential equations whose solutions satisfy the requirements of the extremum of the function *I.* (1) Note that the equations obtained will coincide with Kirchhoff's equations, and this is natural, since the result of the solution should be the same independently of the approach to the solution.

The criterion (3) for Lagrange's function, which was defined for the conservative part of the system, yields the Euler-Lagrange equations.

$$\frac{d}{dt}\left(\frac{\partial \mathfrak{L}}{\partial \dot{q}_j}\right) - \frac{\partial \mathfrak{L}}{\partial q_j} = 0, \tag{6}$$

basing on which it is easy to obtain the above mentioned system of *N* differential equations analogous to Kirchhoff's equations.

Further, it is necessary to take into account the non-conservative forces V_j, which are independent of the generalized coordinates and its momentums (in the case of mechanics). They are considered only as forces applied to the conservative part of the system at the points where these non-conservative forces act. In our case the examples of these forces are the

voltages applied to the clamps of electrical circuits, that is, the Euler-Lagrange equations will take on the form:

$$\frac{d}{dt}\left(\frac{\partial \mathfrak{L}}{\partial \dot{q}_j}\right)-\frac{\partial \mathfrak{L}}{\partial q_j}=V_j \tag{7}$$

In order to take into account the resistance losses, that is, the forces of dissipation in the system, we introduce the Rayleigh function:

$$F=\sum_{j=1}^{N}\frac{1}{2}R_j(\dot{q}_j)^2 \tag{8}$$

Now, finally, for the entire non-conservative system, the Euler-Lagrange equations are written through the conservative Lagrangian as:

$$\frac{d}{dt}\left(\frac{\partial \mathfrak{L}}{\partial \dot{q}_j}\right)-\frac{\partial \mathfrak{L}}{\partial q_j}+\frac{\partial F}{\partial \dot{q}_j}=V_j \tag{9}$$

Note some important features of the approach under consideration to the DC-DC converters dynamics analysis:

1) An important simplification of our analysis is that the Lagrangian is defined only for the conservative part of the circuit.
2) When forming the Lagrangian, for the time being, we may not accentuate our attention on the preserving in an unchanged form the magnitudes of the voltage on the capacitors and the currents trough the inductances, or on their averaging. Indeed, the energies on these elements little differ for both representations of the quantities mentioned. This equivocal attitude towards the form of these quantities can be preserved also on the stage of the formation of the systems of differential equations by the Euler-Lagrange formulas, and it is only at later stages that we will need to clarify that we deal with the averaged quantities. However, to be more specific in the further analysis, we will from the start keep in mind the transition to the averaged quantities without additional changes in the notation of these quantities.
3) The equations of the circuit obtained basing on the Euler-Lagrange equations are linear, thus making it possible to represent the converter in the form of a simple linear circuit whose dynamics coincides with the dynamics of the original converter.
4) The equations obtained are linear, and do not contain commutation functions. The latter were not needed in the course of all the procedures described above. At the same time,

when determining the Lagrangian, we will need to consider the topologies coming into being in the process of the functioning of the converter and to fix on that which defines the trajectory of the system's motion.

5) Note also that when analyzing the system, we will assume that the relations between voltages and currents in the stationary mode are known. As is known, they are derived from the volt-second balance equations of the inductances, or the ampere-second characteristics of the capacitors.

Below, all these assertions are illustrated by many examples.

III. Analysis of the dynamics of the three base DC-DC converters: boost, buck-boost and buck converters.

III-1. Boost converter. The diagram of a classical boost converter is given in Fig. 1a, while the two topologies of its conservative part, in Fig. 1b and 1c. Note that we obtain the conservative part of its design by short-circuiting the voltage source V_{in} and by disconnecting the load R. In the first topology Fig. 1b (the switch is closed, the diode does not conduct) there are no energy changes on the reactive elements, therefore it does not create motion in the interpretation under consideration. The second topology in Fig. 1c (the switch is open, the diode conducts) provides an exchange of energy. The magnetic energy of the inductance $W_q = \frac{(L_{in} i_{in})^2}{2L_{in}}$, but since the average value of current in the topology Fig. 1c in the steady state of an actual converter equals $i = i_{in} D_1$, so by expanding this relation also to the current instant values (as usually is done in the averaging process) $\frac{(L_{in} i_{in})^2}{2L_{in}} = \frac{(Li)^2}{2L}$, where $L = L_{in} / D_1^2$, D, the duty cycle, $D_1 = 1 - D$. Note that the value of the inductance energy did not change. We will call these changes of the inductance current and its value, which occur simultaneously, their reduction to the load. With accounting for the above said, the Lagrangian (3) of the conservative part takes on the form ($v = v_o$).

$$\mathcal{L} = \frac{(Cv)^2}{2C} - \frac{(Li)^2}{2L} \tag{10}$$

Let us write the charge on the capacitor through the derivative of the flux linkage $Cv = -LC\frac{di}{dt}$, then the Lagrangian is $\mathcal{L} = \frac{(LCdi/dt)^2}{2C} - \frac{(Li)^2}{2L}$ (11)

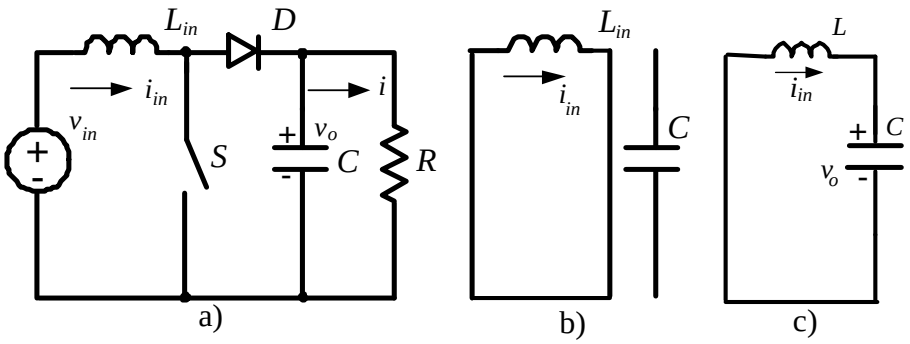

Fig 1: Boost converter, (a) diagram, (b) and (c), the conservative parts of the diagram at the closed and open switch respectively.

1) The transition process under the jump-like action of the input voltage.

Let us perform on (11) the Euler-Lagrange transform according to (6), obtaining ($q = Li$, $C\dot{q} = LC\frac{di}{dt}$).

$$LC\frac{d^2i}{dt^2} + i = 0 \tag{12}$$

Basing on the dimensions in (12), we will assume as the force action the input voltage $\frac{V_o}{R} = \frac{V_{in}}{D_1}\frac{1}{R}$, while the Rayleigh function of the power dissipation will be written in the form $F = \frac{(Cv)^2}{2RC^2} = \frac{1}{2RC^2}\left(LC\frac{di}{dt}\right)^2$. Therefore, on the basis of (9), after dividing all the members of Eq. (12) by LC, we obtain:

$$\frac{d^2i}{dt^2} + \frac{1}{RC}\frac{di}{dt} + \frac{i}{LC} = \frac{V_{in}}{D_1}\frac{1}{RLC} \tag{13}$$

The equation obtained corresponds to the linear diagram in Fig. 2a, the transition process in which – under the jump-like action of the input voltage – in averaged quantities – is in complete correspondence with the transition process in the original boost converter design. While deriving the equation, we neglected the influence of active resistances of the circuit elements, but on the final stage of our analysis, they may be taken into account basing on the energy conversion efficiency of the circuit. The power losses thus obtained make it possible to determine the equivalent input resistance R_{in}, which should be included into the linear diagram in a transformed form, $R_{eq} = R_{in} / D_1^2$, that is, reduced to the load, as the inductance.

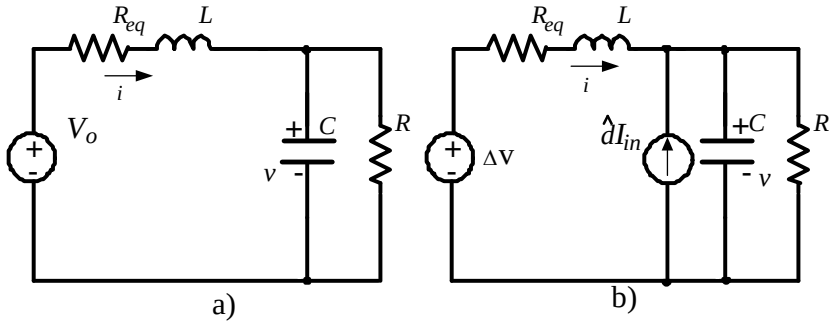

Fig. 2: Equivalent linear diagrams of a boost converter, (a) under jump-like changes of the input voltage, (b) under jump-like changes of the duty cycle.

It should be emphasized, that V_{in} is a function of time - $v_{in}(t)$, and $v_{in}(t) = 0$ at $t < 0$ and $v_{in}(t) = V_{in}$ at $t \geq 0$. This factor is automatically taken into account in modeling the circuit in Fig. 2a and therefore the designation V_{in} will be retained for simplicity. If we analyze the circuit analytically, for example, when solving its equation with respect to the current i, then an impulse function $\delta(t)$ should appear in the derivative.

2) The transient state at jump-like changes of the duty cycle.

Basing on the fact that in (13) $i = i_{in} D_1$, after introducing for the current i_{in} small changes $\hat{i}_{in}$ and, for the duty cycle D, its increment $\hat{d}$, we get.

$$i = (I_{in} + \hat{i}_{in})(D_1 - \hat{d}) = I_{in} D_1 - I_{in}\hat{d} + \hat{i}_{in}(D_1 - \hat{d}) = I_{in} D_1 - I_{in}\hat{d} + \hat{i} \qquad (13a)$$

We also take into account that a change of the duty cycle D will also cause a change in the input action in (13) by the quantity ΔV.

$$\Delta V = \frac{V_{in}}{D_1 - \hat{d}} - \frac{V_{in}}{D_1} = \frac{V_{in}\hat{d}}{D_1(D_1 - \hat{d})} \qquad (14)$$

Now (13) is being transformed into the form, which makes it possible to determine the transition process at a jump-like change of D:

$$\frac{d^2\hat{i}}{dt^2} + \frac{1}{RC}\frac{d\hat{i}}{dt} + \frac{\hat{i}}{LC} = \frac{V_{in}\hat{d}}{D_1(D_1 - \hat{d})}\frac{1}{RLC} + \frac{I_{in}\hat{d}}{LC} \qquad (14a)$$

When obtaining this equation we took into account that $\frac{I_{in} D_1}{LC} = \frac{V_{in}}{D_1}\frac{1}{RLC}$, and these member cancel each other out. Besides, the value of the inductance in (14) with the change in D

should also be changed: $L = L_{in}/(D_1 - \hat{d})^2$. All that has been said above regarding the function V_{in} equally applies to the value $I_{in}\hat{d}$.

Eq. (14) is in correspondence with the linear diagram in Fig. 2b, whose transition process under the jump-like action of the duty cycle is also in full correspondence in averaged values with the transition process in the initial circuit of the boost converter. In the two previous approaches to the analysis of transient states, for simplicity sake, we also spoke of a jump-like action of the input voltage, or the duty cycle, however, the analysis will remain unchanged if these actions are functions of time. Note that Eqs. (13) and (14a) may be – as is usually done – subjected to the Laplace transform to describe a system of automatic control. We do not consider these procedures due to their trivial character.

III-2. Buck-boost converter

The diagram of a classic buck-boost converter is given in Fig. 3a. Obviously, the conservative part of the diagram in the two possible topologies will completely coincide with the latter for the boost converter in Fig. 1b,c. This means that the Lagrangians (10) and (11) remain valid in this case also, therefore the concluding Eq. (13) preserves its form, differing only in that, in order to preserve the actual value of the current through the load R, the power action – the input voltage – should be chosen equal to $\frac{V_{in}D}{D_1}$, that is,

$$\frac{d^2 i}{dt^2} + \frac{1}{RC}\frac{di}{dt} + \frac{i}{LC} = \frac{V_{in}D}{D_1}\frac{1}{RLC} \tag{15}$$

Obviously, this equation describes the transient state under the action of the input voltage.

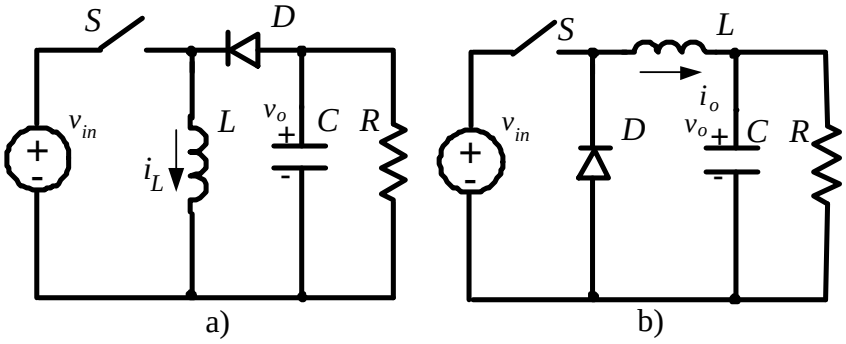

Fig. 3: (a) boost converter, (b) buck converter.

Since Eq. (15) for the buck-boost converter differs from (13) only by the right-hand part, then in the mode of the action by the duty cycle, Eq. (14) remains in general preserved also for the buck-boost converter differing only by that instead of $I_{in}\hat{d}/LC$ there should be inserted the expression $I_L\hat{d}/LC$.

The value $\frac{V_{in}\hat{d}}{D_1(D_1-\hat{d})}\frac{1}{RLC}$ has been preserved:

$\Delta V\frac{1}{RLC}=\left(\frac{V_{in}(D+\hat{d})}{D_1-\hat{d}}-\frac{V_{in}D}{D_1}\right)\frac{1}{RLC}=\frac{\hat{d}V_{in}}{D_1(D_1-\hat{d})}\frac{1}{RLC}$, that is.

$$\frac{d^2\hat{i}}{dt^2}+\frac{1}{RC}\frac{d\hat{i}}{dt}+\frac{\hat{i}}{LC}=\frac{\hat{d}V_{in}}{D_1(D_1-\hat{d})}\frac{1}{RLC}+\frac{I_L\hat{d}}{LC} \quad (16)$$

With accounting for this change of the source of current, the linear diagrams in Fig. 2a,b also keep their forms.

III-3. Buck converter

This converter (Fig. 3b) is a rather simple one from the point of view of the analysis of dynamics. In a purely formal approach, Eqs. (4)-(8) are being preserved, while in Eq. (9) the force action should obviously equal $V_j = DV_{in}$, that is, Eq. (13) takes on the form.

$$\frac{d^2i}{dt^2}+\frac{1}{RC}\frac{di}{dt}+\frac{i}{LC}=\frac{DV_{in}}{RLC} \quad (17)$$

and all the parameters of the diagram remain unchanged. Upon changing the duty cycle *D* for a new transient state, we get:

$$\frac{d^2\hat{i}}{dt^2}+\frac{1}{RC}\frac{d\hat{i}}{dt}+\frac{\hat{i}}{LC}=\frac{\hat{d}V_{in}}{RLC} \quad (18)$$

IV. Analysis of the dynamics of three hybrid DC-DC converters: Cuk, Sepic and Zeta converters

Analyzing the dynamics of these converters using the Lagrangian is of special interest, since these convertors contain four reactive elements, and analyzing them using usual methods leads to rather cumbersome formulae and non-transparent results.

IV-1. Cuk converter. Fig. 4a shows the full diagram of the converter, while Fig. 4b, c, the conservative parts of its two topologies. The first topology is formed for the conductance of

the diode D_o and shows the relations of the energies of the components L_1 and C_1, while the second, for the conductance of the switch S, and shows the connection between the energies of the elements L_2, C_1 and C_2. This topology is a generalization of the right-hand part of the diagram in Fig. 4b, therefore, this right-hand part with the elements L_2, C_2 is left out of consideration. In Fig. 4b the current i_1 is the input current i_{in} reduced to the load, that is, $i_1 = i_{in}/(D/D_1)$, and the voltage $v_1 = vD$ also is the voltage on the capacitor C reduced to the load. Clearly, in order to preserve the energy on these components, the values of the inductance L_{in} and the capacitance C: $L_1 = L_{in}(D/D_1)^2$ and $C_1 = C/D^2$, should also be changed. In Fig. 4b,c indices of other values have also been changed, which themselves do not change.

1) Transient response upon jump-like actions of the input voltage. Basing on the diagrams in Fig. 4b,c we write the values of the magnetic and electric energies of the conservative part of the converter. We take the flux linkages $L_1 i_1$ and $L_2 i_2$, as the generalized coordinates q_j, like we did it in Section 3, while the voltages on the capacitors yield their derivatives $\dot{q}_j$ and, respectively, the charges on the converters $C_1 v_1$ and $C_2 v_2$. With accounting for this,

$$W_q = \frac{(L_1 i_1)^2}{2L_1} + \frac{(L_2 i_2)^2}{2L_2} \tag{19}$$

$$W_{\dot{q}} = \frac{(C_1 v_1)^2}{2C_1} + \frac{(C_2 v_2)^2}{2C_2} \tag{20}$$

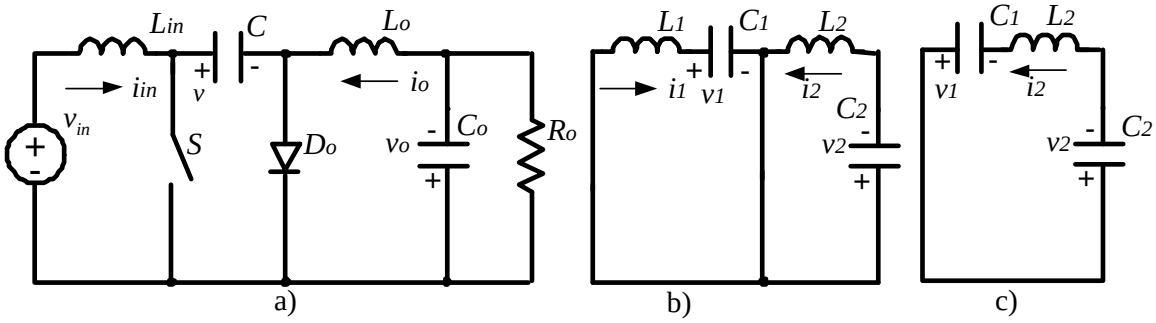

Fig. 4: Cuk converter, (a) diagram, (b) and (c), the conservative parts of the diagram at the open and closed switch respectively.

Further, we express the charges on the capacitors through the derivatives of the flux linkages. From Fig. 4b we find $C_1 v_1 = -L_1 C_1 \frac{di_1}{dt}$, and from Fig 4c, $C_2 v_2 = -L_1 C_2 \frac{di_1}{dt} - L_2 C_2 \frac{di_2}{dt}$. Thus, the sought Lagrangian takes on the form:

$$\mathcal{L} = \frac{(L_1 C_1 (di_1/dt))^2}{2C_1} + \frac{(L_1 C_2 (di_1/dt) + L_2 C_2 (di_2/dt))^2}{2C_2} - \frac{(L_1 i_1)^2}{2L_1} - \frac{(L_2 i_2)^2}{2L_2} \tag{21}$$

Basing on the Euler-Lagrange equations, we obtain two equations of the conservative part:

$$L_1 C_1 \frac{d^2 i_1}{dt^2} + i_1 - i_2 = 0$$

$$L_1 C_2 \frac{d^2 i_1}{dt^2} + L_2 C_2 \frac{d^2 i_2}{dt^2} + i_2 = 0 \tag{22}$$

As the energy function of power dissipation, we take the following equality.

$$F = \frac{(C_2 v_2)^2}{2RC_2^2} = \frac{1}{2RC_2^2}\left(L_1 C_2 \frac{di_1}{dt} + L_2 C_2 \frac{di_2}{dt} \right)^2 \tag{23}$$

Action of forces will be determined by the output voltage of the converter divided by the resistivity of the load, $\frac{V_{in} D}{D_1} \frac{1}{R} = \frac{V_o}{R}$. In the end, the equations for the averaged values of the currents i_1 and i_2 take on their final form.

$$L_1 C_1 \frac{d^2 i_1}{dt^2} + i_1 - i_2 = 0$$

$$L_1 C_2 \frac{d^2 i_1}{dt^2} + L_2 C_2 \frac{d^2 i_2}{dt^2} + \frac{L_1}{R}\frac{di_1}{dt} + \frac{L_2}{R}\frac{di_2}{dt} + i_2 = \frac{V_o}{R} \tag{24}$$

The linear diagram given in Fig. 5a corresponds to this equations system. So, Eqs. (24) and the linear diagram in Fig. 5a are a solution of the problem of describing transient states in a Cuk converter upon a jump-like change of the input voltage.

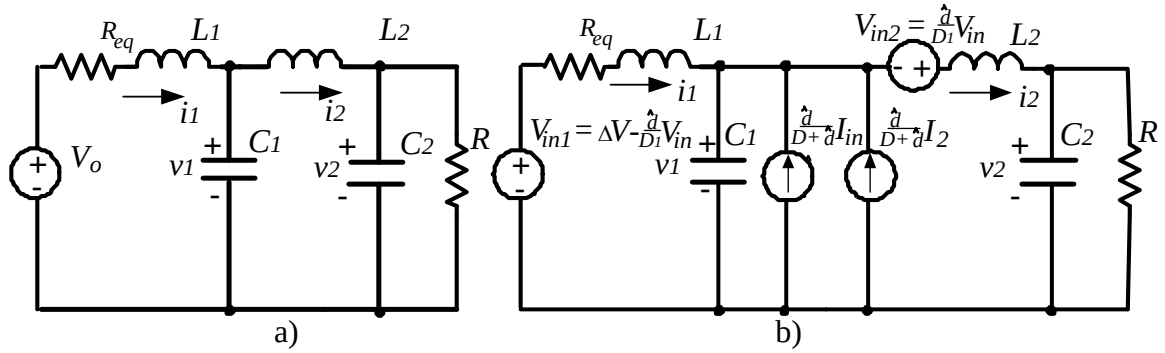

Fig. 5: Equivalent linear circuit of a Cuk converter, (a) under jump-like changes of the input voltage, (b) under jump-like changes of the duty cycle.

2) Transient response upon jump-like changes of the duty cycle. Let us introduce small increments into the first of Eqs. (22), and, replacing the current i_1 with $i_1 = i_{in}/((D+\hat{d})/(D_1-\hat{d}))$, as well as taking into account the changed values of $L_1 = L_{in}((D+\hat{d})/(D_1-\hat{d}))^2$ and $C_1 = C/(D+\hat{d})^2$, we get:

$$(D+\hat{d})L_1C_1\frac{d^2\hat{i}_1}{dt^2}+(I_{in}+\hat{i}_{in})(D_1-\hat{d})-(I_2+\hat{i}_2)(D+\hat{d})=0 \qquad (25)$$

Since for a Cuk converter $I_{in}D_1 = I_2D$ and also $\hat{i}_{in}/((D_1-\hat{d})/(D+\hat{d})) = \hat{i}_1$, we finally get:

$$L_1C_1\frac{d^2\hat{i}_1}{dt^2}+\hat{i}_1-\hat{i}_2=\frac{I_{in}\hat{d}}{D+\hat{d}}+\frac{I_2\hat{d}}{D+\hat{d}} \qquad (26)$$

Thus, with the help of this equation, we have taken into account the initial values of the currents i_1 and i_2 on the inductances by the moment of the change of the duty cycle. However, the circuit also contains two capacitors, and we must also take into account the initial values of the voltages on them. To do that, we take the linear circuit in Fig. 5a and write two equations through the voltages on the capacitors:

$$\begin{aligned} L_1\frac{di_1}{dt}+v_1&=V_o,\\ L_2\frac{di_2}{dt}+v_2-v_1&=0 \end{aligned} \qquad (27)$$

Let us introduce small increments into the first equations in (27) replacing the voltage v_1 with $v_1 = vD$, and taking into account that in the steady-state the voltage on the capacitor $C, V = V_{in}/D_1$, and in an equivalent circuit in Fig. 5a, $V_1 = V_{in}D/D_1$, we get:

$$L_1\frac{d\hat{i}_1}{dt}+\left(\frac{V_{in}}{D_1}+\hat{v}\right)(D+\hat{d})=V_o+\Delta V \tag{28}$$

Accounting also for $\frac{V_{in}D}{D_1}=V_o$, $\Delta V=\frac{V_{in}(D+\hat{d})}{D_1-\hat{d}}-\frac{V_{in}D}{D_1}=\frac{V_{in}\hat{d}}{D_1(D_1-\hat{d})}$ and $\hat{v}_1=\hat{v}(D+\hat{d})$, Eq. (28) takes on the form.

$$L_1\frac{d\hat{i}_1}{dt}+\hat{v}_1=\frac{V_{in}\hat{d}}{D_1(D_1-\hat{d})}-\frac{V_{in}\hat{d}}{D_1} \tag{29}$$

Treating the voltage v_1 in the second equation in (27) in the very same manner, we get

$$L_2\frac{d\hat{i}_2}{dt}+\hat{v}_2-\hat{v}_1=\frac{V_{in}\hat{d}}{D_1} \tag{30}$$

Eqs. (26), (29), (30) are in correspondence with the linear diagram in Fig. 5b, which is totally equivalent to the Cuk converter as concerns the course of its dynamic mode upon jump-like changes of the duty cycle.

IV-2. Sepic converter. Fig. 6a shows the complete design of the converter, while Fig. 6b shows the conservative part of its topology, which combines the energy exchanges on the conductance interval of the diode D_o and on the interval of the closed state of the switch *S*. As in the case of the Cuk converter, in Fig. 6b the current i_1 is the input current i_{in} reduced to the load, that is, $i_1=i_{in}/(D/D_1)$, while the voltage $v_1=v(D/D_1)$ also is the voltage on the capacitor *C* reduced to the load. For the preservation of energy on these components the values of inductance, L_{in}, and the capacitor, *C*, should also be changed: $L_1=L_{in}\cdot(D/D_1)^2$ and $C_1=C/(D/D_1)^2$. The notation L_o, C_o are replaced with L_2, C_2.

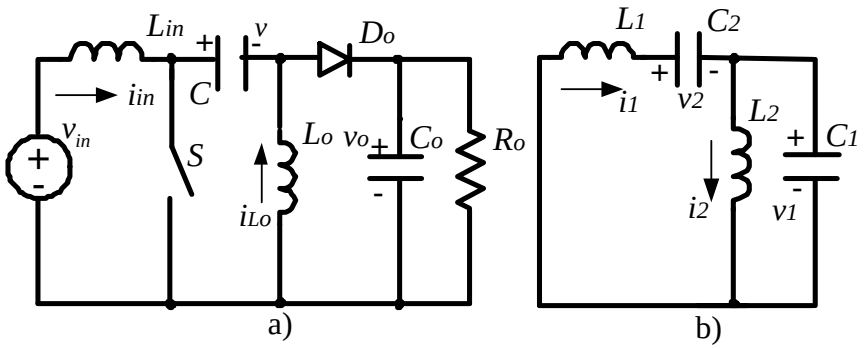

Fig. 6: Sepic converter, (a) circuit, (b) the conservative part of the diagram at the closed and open switch.

1) Transient state upon jump-like changes of the input voltage. As in previous sections, with accounting for the preservation of the form of the generalized coordinates Eqs. (19) and (20) for the values of the magnetic and electrical energies of the conservative part of the converter (Fig. 6) remain unchanged. And we find the charges on the capacitors through the derivatives of the flux linkages from Fig. 6b: $C_1 v_1 = L_2 C_1 \frac{di_2}{dt}$ and $C_2 v_2 = -L_1 C_2 \frac{di_1}{dt} - L_2 C_2 \frac{di_2}{dt}$.

Thus the sought Lagrangian takes on the form

$$\mathcal{L} = \frac{(L_2 C_1 (di_2/dt))^2}{2C_1} + \frac{(L_1 C_2 (di_1/dt) + L_2 C_2 (di_2/dt))^2}{2C_2} - \frac{(L_1 i_1)^2}{2L_1} - \frac{(L_2 i_2)^2}{2L_2} \tag{31}$$

On the basis of the Euler-Lagrange equations, we get two equations of the conservative part.

$$L_2 C_1 \frac{d^2 i_2}{dt^2} + i_2 - i_1 = 0$$

$$L_1 C_2 \frac{d^2 i_1}{dt^2} + L_2 C_2 \frac{d^2 i_2}{dt^2} + i_1 = 0 \tag{32}$$

We still take Eq. (33) as the energy function F of the power dissipation, and $\frac{V_{in} D}{D_1} \frac{1}{R} = \frac{V_o}{R}$ as the force action. As a result, the equations for the determining the averaged values of the currents i_1 and i_2 upon jump-like actions of the input voltage take on the final form

$$L_2 C_1 \frac{d^2 i_2}{dt^2} - i_1 + i_2 = 0$$

$$L_1 C_2 \frac{d^2 i_1}{dt^2} + L_2 C_2 \frac{d^2 i_2}{dt^2} + \frac{L_1}{R} \frac{di_1}{dt} + \frac{L_2}{R} \frac{di_2}{dt} + i_1 = \frac{V_o}{R} \tag{33}$$

This system of equation is in correspondence with the linear circuit in Fig. 7a. As compared with Fig. 5a, the inductances L_1 and L_2 switched places.

2) Transient state upon jump-like changes of the duty cycle.

Transforming Eqs. (32), (33) by analogy with the transformations(25)-(30), we will get for this mode an equivalent linear circuit in Fig. 7b. Eq. (33) differs from (34) in the signs at the currents i_1, i_2, as well as in the value of the voltage on the capacitor C_1 in the steady state mode in the Sepic converter: $V_c = V_{in}$. Therefore, we have obtained relevant linear circuits both in the case of the transient state upon changes of the input voltage and in the case of changes in the duty cycle.

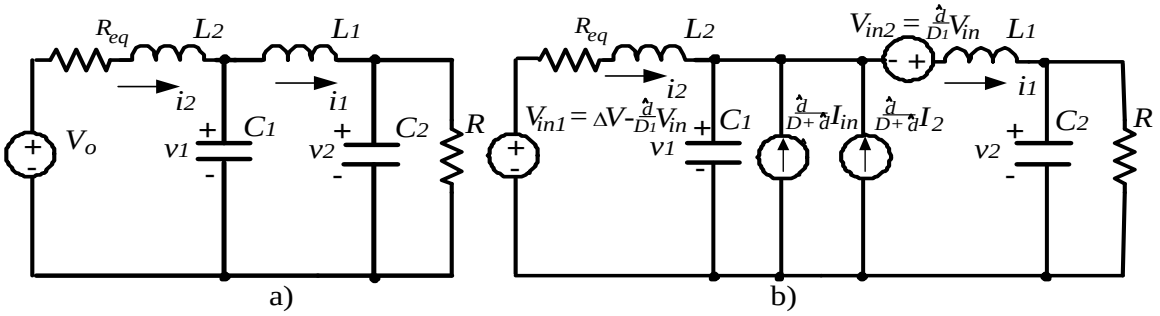

Fig. 7: Equivalent linear circuits of a Sepic converter, (a) under jump-like changes of the input voltage, (b) under jump-like changes of the duty cycle.

IV-3. Zeta converter. Fig. 8a gives the full circuit of the converter, and Fig. 8b,c, the conservative parts of its two topologies: for the conductance of the diode D_o and for the case of the closed switch *S*.

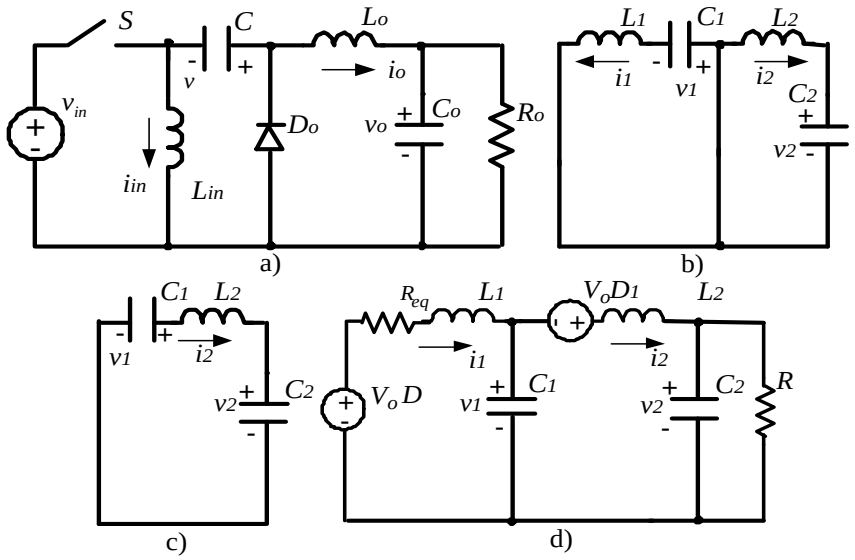

Fig. 8: Zeta converter, (a) circuit, (b) and (c), the conservative parts of the circuit at the open and closed switch respectively, (d) the equivalent circuit under jump-like changes of the input voltage.

The first topology represents the relation of the energies of the components L_1 and C_1, and the second – upon the conductance of the switch *S* – represents the connection of the energies of the components L_2, C_1 and C_2. This topology is a generalization of the right-hand part of the diagram Fig. 8b, so we do not consider this right-hand part with components L_2 and C_2. In Fig. 8b the current i_1 is the input current i_{in} reduced to the load, that is, $i_1 = i_{in}/(D/D_1)$, and, as before, $L_1 = L_{in} \cdot (D/D_1)^2$.

As a result, we see a full analogy with the processes in a Cuk converter, thus making it possible to base on the system of equations(22) in our further analysis. The equation of the energy function of power dissipation(23) also remains unchanged. However, in this case, as can be seen from the operation principle of the Zeta converter, the force effect acts only on the interval of the closed switch (interval *D*), i.e., in the mode of jump-like action of the input voltage, it should be equal to V_oD. But since the output voltage in the equivalent circuit must remain V_o, it is necessary to introduce an additional source V_oD_1 which applied to the circuit L_2-C_2||R-C_1. This makes it possible to represent an equivalent linear circuit for the Zeta converter in this mode as is shown in Fig. 8d. Since the voltage across the capacitor C is $v = V_o$, the condition $C_1 = C / D^2$ must be satisfied to conserve its energy in the equivalent circuit.

For jump-like changes of the duty cycle, the input source is already divided into two parts, as follows from Fig. 5b. The values and the mode of the activating of the sources of current, determined by the first equations of systems(22,23), remain unchanged. Therefore, the diagram in Fig. 5b will serve as an equivalent linear circuit of the Zeta converter in the mode of jump-like changes of the duty cycle.

V. Dynamics analysis of some DC-DC converters with an improved output voltage gain.

In the last decades, the main direction of new solutions in the field of DC-DC converters consisted in improving the output voltage gain both in the buck- and especially, in the boost converters. It dictated the introduction in the circuit of additional components, including inductors and capacitors. As a result, the orders of the differential equations of these converters increased, leading, in particular, to difficulties in analyzing dynamic modes making them more cumbersome and less transparent.

The designs with magnetically connected inductors, with voltage multipliers, and with switched-capacitor/switched-inductor blocks became the mainstream directions in increasing the output voltage gain. Below we will quote some examples of the dynamics analysis of such enhanced converters basing on energy functions. The diagrams of these converters are shown in Fig. 9.

Previously, on the basis of the Euler-Lagrange equations, using the Lagrangians, we got linear circuits described by identical dynamics under the action of the input voltage. In order

to get a linear circuit describing the dynamic state upon changes in the duty cycle, we needed to get another circuit with the sources of voltage and current, which take into account the initial conditions at the moment of the change of the duty cycle (see, for instance Fig. 5). We emphasize that like in the case of the boost converter in Section III-1 where an equivalent linear circuit of Fig. 2a was obtained, alike for the same linear circuit, on the contrary, can be set in correspondence with a conventional boost converter with the identical dynamics, both upon the action of the input voltage and changes in the duty cycle – without any changes of its parameters. Thus, more complex circuit of enhanced boost converters are reduced to the circuit on an equivalent conventional boost converter, with well-known dynamics. Consider this in more detail on four examples from Fig. 9. We will keep in mind the following notation of the parameters of the said boost converter: the input voltage v_{in}, the input inductor L, its current i, the capacitor C, load R and its output voltage v.

V-1. Fig. 9a gives the diagram of a modification of the boost converter with magnetically connected inductors L_1 and L_2, so that $L_2=n^2L_1$ and n is the ratio of the turns of these inductors.[5] An additional diode D_1 is designated for transmitting the dissipation inductance current to the load for the linkage coefficient $k<1$. For simplification and illustration, in this analysis we assume $k=1$, which yields $V_{out}=V_{in}(1+nD)/(1-D)$. In order to write a Lagrangian, as before, we will take the flux linkage of the inductor as a generalized coordinate, and the charge of the capacitor as its "momentum". This makes it possible to write the magnetic and electrical energies of the diagram, and respectively, its Lagrangian: $\mathcal{L}=(LCdi/dt)^2/2C-(Li)^2/2L$. It is seen from the Lagrangian that the equivalent inductance of the conventional boost converter must be $L=L_1(n+1)^2$, its input voltage source, $v_{in}=V_{in}(1+nD)$, and all the other parameters remain unchanged: $C=C_o$, $R=R_o$. This we have obtained the design of a simple conventional boost converter with exactly the same dynamics of averaged values as in the far more complex original converter.

V-2. Fig. 9b shows a widespread modification of the boost converter with a voltage multiplier based on the Dickson multiplier with three links (Axelrod, et. al., 2015). In such a converter with N links $V_{out}=V_{in}(N+1)/(2(1-D))$. Since, as is known, in such a design the voltages on the capacitors $|v_1|=|v_2|=V_{in}/(1-D)$, $|v_3|=|2v_1|$, that is, the output voltage in this example $v_o=2v_1$, then at $C_1=C_2=C_3=C_o$ the sum of energy on the capacitors, that is, electrical

energy, equals $W_{\dot{q}} = (3/2)C_o v_o^2$. Since it is necessary to increase the input voltage in a conventional boost converter by the factor of $(N+1)/2 = 2$, and respectively to decrease by the factor of two the input current, for energy conservation sake, the inductance in it must be increased by the four times. The Lagrangian will take the form as in paragraph V-1, where $C = (3/2)C_o$, $L = \left(N/2\right)^2 \cdot L_{in} = 4L_{in}$ and $v_{in} = V_{in}((N+1)/2) = 2V_{in}$. Also in that case of a rather complex design, we come to a less complex converter with the identical dynamics due to the choice of a correct energy function. Note that the number of links (three) in that example is not of paramount importance, since it, with correct accounting for the equivalent electrical energy, may be arbitrarily large.

V-3. The Fig. 9c gives the design of a boost converter with a switched-inductor block, which makes it possible to get the output voltage $V_{out} = V_{in}(1+D)/(1-D)$ (Axelrod, et. al., 2020). For $i_1 = i_2 = i$, $L_1 = L_2 = L_o$, the magnetic energy of the design is $W_q = L_o i^2$, while the corresponding Lagrangian also will take the form as in paragraph V-1. Obviously, the dynamics of the initial converter may be assessed by an equivalent boost converter whose input inductance equals $L = 2L_o$, and the input voltage $v_{in} = V_{in}(1+D)$. In that example the input inductance is split into two parts, but our approach to the analysis will not change if it is split into *N* parts.

V-4. As the last example, consider a boost converter with a switched-capacitor block, which also makes it possible to get the output voltage $V_{out} = V_{in}(1+D)/(1-D)$ (Axelrod, et. al., 2020). To the conservative part of that design at the open switch, one can put into correspondence a Lagrangian.

$\mathcal{L} = (L_1 C_1 di_1/dt)^2/2C_1 + (L_1 C_2 di_1/dt + L_2 C_2 di_2/dt)^2/2C_2 - (L_1 i_1)^2/2L_1 - (L_2 i_2)^2/2L_2$, (its parameters are explained below). Basing on it, we will write the Euler-Lagrange equations and obtain a linear design structurally coinciding with the design of the converter (naturally, without the switches and diodes, and with one capacitor instead of two, C_a and C_b: as in the second example, we accept the notation $C_a = C_b = C$). It coincides with Fig. 5a with the parameters $L_1 = L_{in}((1+D)/(1-D))^2$, $C_1 = 2C/(1+D)^2$ and unchanged L_2=L_o, $C_2 = C_o$ and R= R_o. Since the original converter is based on the boost converter, so, as is shown in (Axelrod, et. al., 2020), this linear design can be simplified: the capacitors C_1 and C_2 can be

united, and the inductances L_1 and $L_2' = L_2/(1+D)^2$ can also be united, where the latter is reduced to the former's current, thus as a result, in an equivalent linear diagram $L_{12} = L_1 + L_2'$ and $C_{12} = C_1 + C_2$.

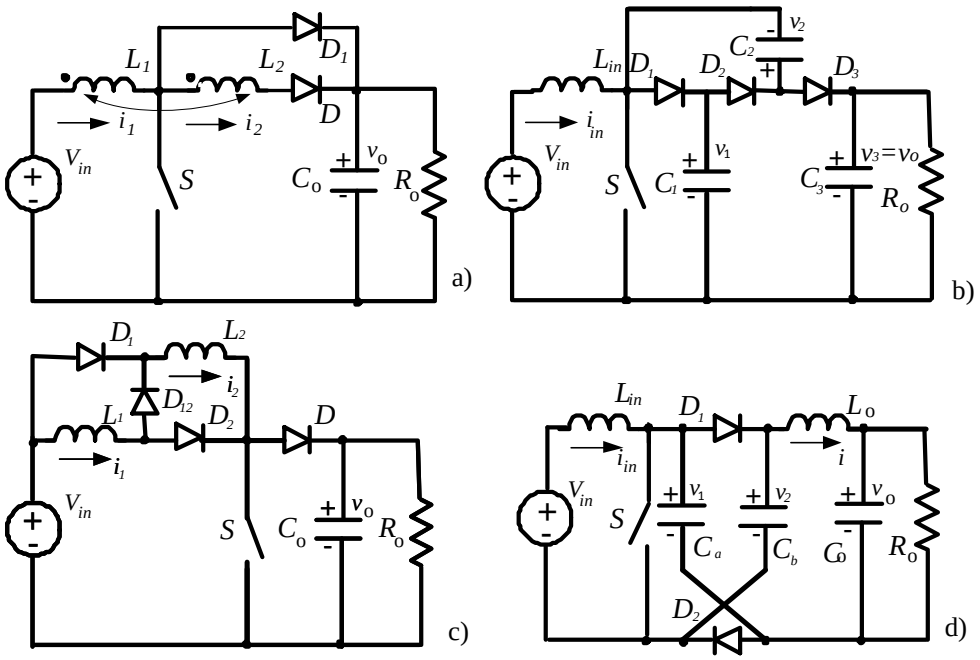

Fig. 9: The diagrams of four enhanced converters.

In its turn, this three-element design can be put in correspondence with a conventional boost converter whose dynamics would be identical to the original more complex design, in which $v_{in} = V_{in}(1+D)$, inductance $L = L_{12}(1-D)^2$, output capacitor $C = C_{12}$ and load R.

VI. Simulation and experiment results

In order to check the results of the theoretical analysis, we carried out modeling in PSPICE of the transient states for all the converters considered above. The parameters of the modeled circuit for six types of classic converters are given in Attachment in Table 1A, while the modelling results, in Fig. 10. Respectively, the parameters of the modeled circuit of Fig. 9 for four types of converters with an improved the output voltage gain are shown in Table 2A, while the modeling results, in Fig. 11.

For all the converter types in Fig. 10, we carried out the testing of the converter switching under consideration to the voltage V_{in} at the duty cycle $D=0.5$, with fixing the curves of the input inductance current i_{in} and the output voltage v_o. Then the duty cycle was jump-like

changed until reaching the value *D=0.75*, with continued fixing of the same values. Simultaneously, for *D=0*.5, we checked the curves of the input inductance *i* and the output voltage *v* for an equivalent linear circuit valid for jump-like changes of the input voltage, and for *D=0.75*, - for an equivalent linear circuit valid for jump-like changes of the duty cycle from *D=0.5* to *D=0.75*.

In the cases of the Cuk, Sepic and Zeta converters, we measured the currents of the input and output inductances i_{in}, i_o, and output voltage v_o, and in the equivalent linear circuit, the currents of two inductances: the current i_1 on the input side, and the current i_2 on the output side, as well as the voltages on the output capacitor, v_2. In all the computer oscillograms we used the same color designation for the curves obtained: i_{in} – green, i (or i_1) - red, v_o - blue, v (or v_2) -purple, i_o – brown and i_2 - yellow.

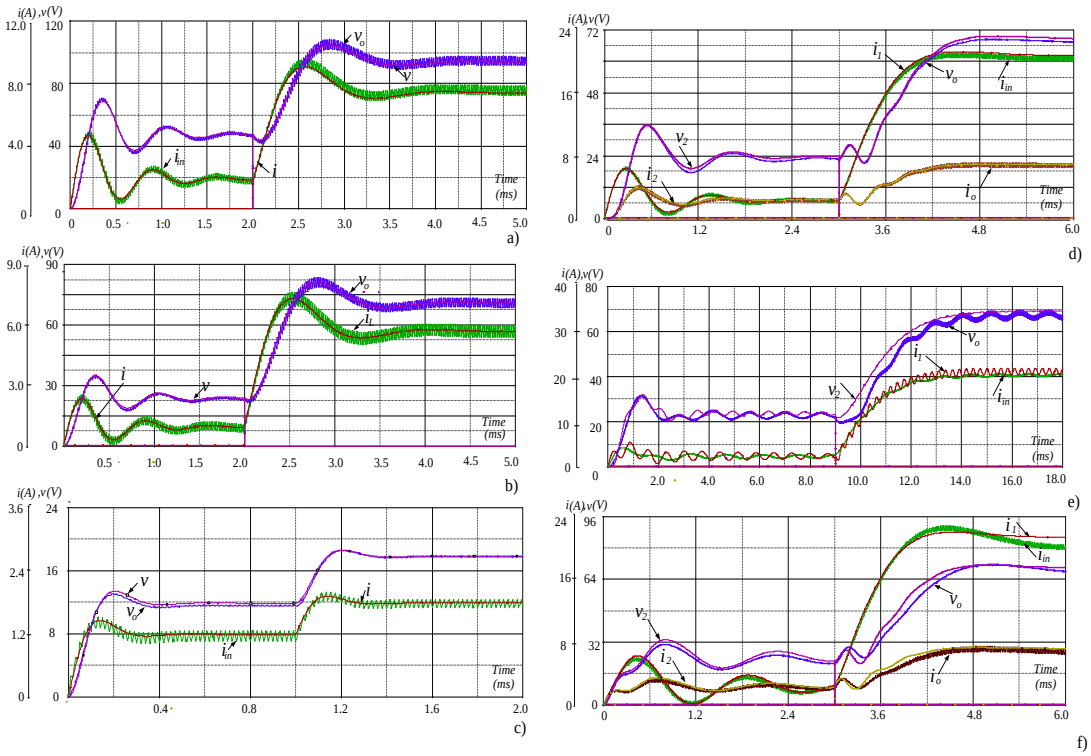

Fig 10: Modeling in PSPICE of the transient states for six types of classic converters, (a) boost, (b) buck-boost, (c) buck, (d) Cuk, (e) Sepic, (f) Zeta.

Fig. 11 gives the results of the testing of the converters from Fig. 9 in the same modes of switching to the input voltage V_{in} at the duty cycle *D=0.5* followed by a jump-like transition to the duty cycle *D=0.75*. In that case, the comparison was carried out with the processes in an equivalent boost converter. For a design under consideration, we measured the current in

the input inductance i_{in} and the output voltage v_o. Note that for the design in Fig. 9a we used the averaged value of the inductance L_1 current, and for the design of Fig. 9c, the current in one of the inductances (the currents in both equal).

In the model of an equivalent boost converter, we measured the current i of the inductance, and the output voltage v. The colors of the curves remained unchanged. The modeling results show that in all the cases considered there was observed a good coincidence transient states of the currents and voltages curves with the corresponding values in the equivalent linear circuits or with the values in an equivalent boost converter.

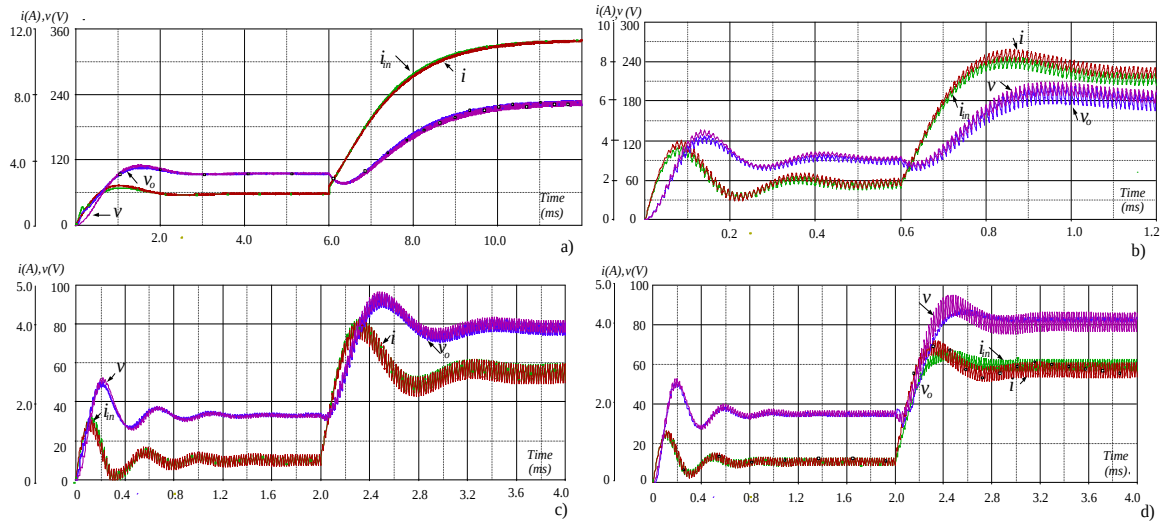

Fig. 11: Modeling in PSPICE of the transient states for four enhanced converters of Fig. 9, (a), (b), (c), (d) –converters Fig. 9a, b, c, d respectively.

We carried out experimental testing of the theoretical results on physical models of two types of converters, from basic groups in Sections III and IV, namely, the buck-boost converter and the Cuk converter. The parameters of the converters and the notation of the curves observed coincided with their values and notation upon the simulation. The results of the testing are given in the oscillograms in Figs. 12, which show the transient states when the converter under consideration is activated for D=0.5, and for the activation of the same voltage of the equivalent linear circuit valid for jump-like changes of the input voltage of the original converter. As is seen from the oscillograms, the curves illustrate the identity of the course of transient states in the converter under consideration and in an equivalent linear circuit.

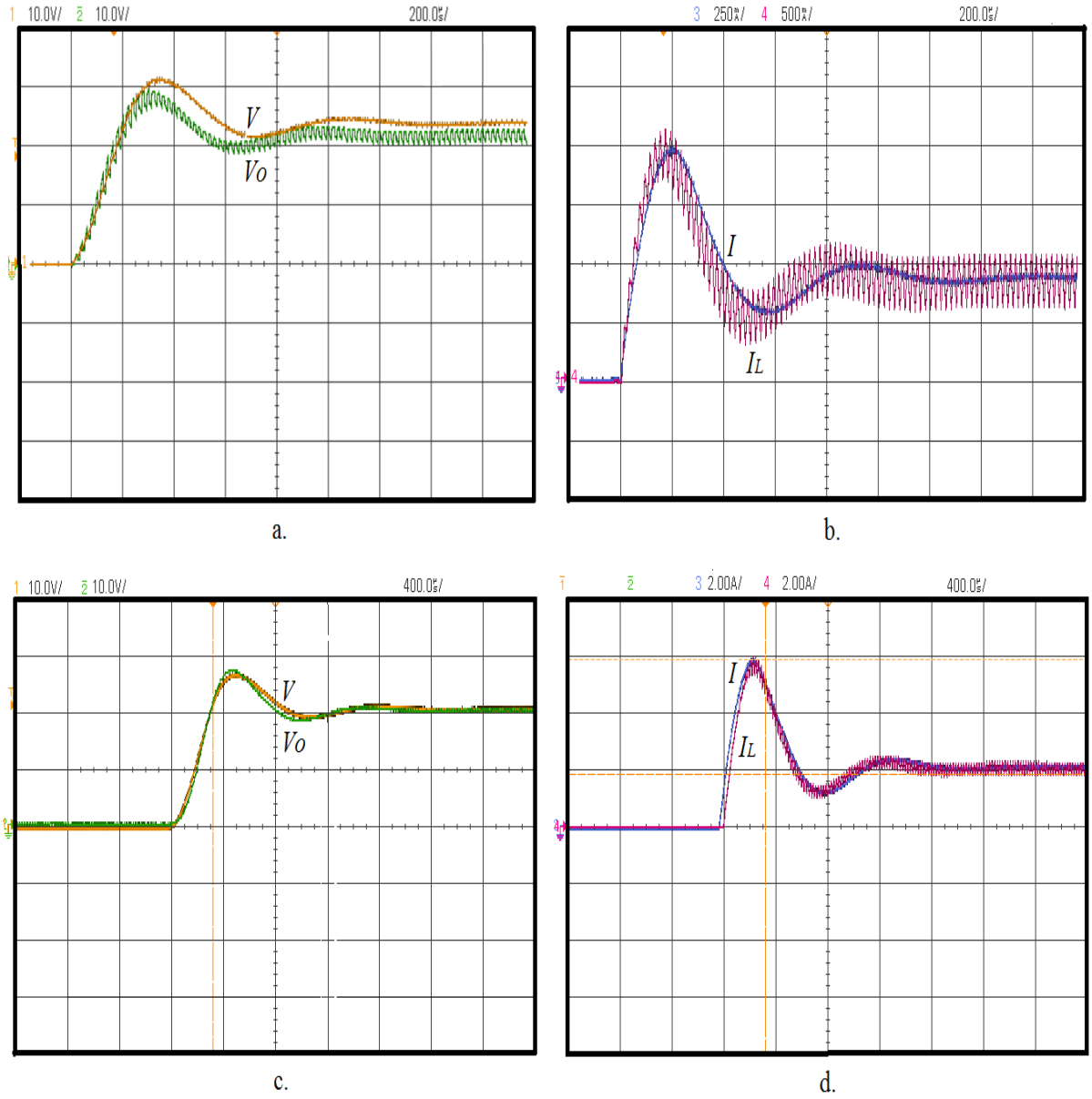

Fig 12: The process of switching on the investigated converters with a duty cycle of D = 0.5 and their equivalent linear analogs, (a), (b) buck-boost converter, (c), (d) Cuk converter.

Attachment

Table 1: A.

Con-verter	**Parameters of initial converter**	**Parameters of first equivalent linear circuit**	**Parameters of second equivalent linear circuit**
Boost, Fig.1, 2	$V_{in}=24V \;\; L_{in}=0.6mH \;\; C=5\mu F \;\; R=50\Omega$	$D=0.5 \;\; V_{in}=48V \;\; L=2.4mH$ $C=5\mu F \;\; R=50\Omega$	$D=0.75 \;\; V_{in}=48V \;\; \hat{dI}_{in}=0.5A \;\; L=9.6mH \;\; C=5\mu F \;\; R=50\Omega$
Buck-boost	The parameters are the same.	The parameters are the same, except $V_{in}=24V$	The parameters are the same, except $\hat{dI}=0.25A$
Buck	The parameters are the same, except $R=10\Omega$.	The parameters are the same, except for $D=0.5 \;\; V_{in}=12V$, for $D=0.75$ $V_{in}=18V$	
Cuk	$V_{in}=24V \;\; L_{in}=L_o=0.6mH$ $C=10\mu F \;\; C_o=10\mu F \;\; R_o=10\Omega$	$D=0.5$ $V_{in}=24V \;\; L_1=L_2=0.6mH \;\; C_1=40\mu F$ $C_2=10\mu F \;\; R=10\Omega$	$D=0.75 \;\; V_{in1}=36V \;\; V_{in2}=12V \;\; I_1=I_2=0.8A \;\; L_1=5.4mH \;\; L_2=0.6mH$ $C_1=18\mu F \;\; C_2=10\mu F \;\; R=10\Omega$
Sepic	$V_{in}=24V \;\; L_{in}=2mH$ $L_o=1mH \;\; C=20\mu F \;\; C_o=50\mu F \;\; R_o=10\Omega$	$D=0.5 \;\; V_{in}=24V \;\; L_1=2mH$ $L_2=1mH \;\; C_1=20\mu F \;\; C_2=50\mu F \;\; R=10\Omega$	$D=0.75 \;\; V_{in1}=36V \;\; V_{in2}=12V \;\; I_1=I_2=0.8A \;\; L_1=18mH \;\; L_2=1mH$ $C_1=2\mu F \;\; C_2=50\mu F \;\; R=10\Omega$
Zeta	$V_{in}=24V \;\; L_{in}=L_o=0.6mH$ $C=20\mu F \;\; C_o=10\mu F \;\; R=10\Omega$	$D=0.5 \;\; V_{in1}=12V \;\; V_{in2}=12V \;\; L_1=L_2=0.6mH$ $C_1=80\mu F \;\; C_2=10\mu F \;\; R=10\Omega$	The parameters of Cuk converter for $D=0.75$

Table 2A.

Con-verter	Parameters of initial converter	Parameters of equivalent boost converter
Fig. 9a	$V_{in}=24V\ L_1=2.4mH\ L_2=9.6mH\ C_o=2\mu F\ R_o=200\Omega$	$V_{in}=48(60)V\ L=21.6mH\ C=2\mu F\ R_o=200\Omega$
Fig. 9b	$V_{in}=24V\ L_{in}=0.6mH$ $C_1=C_2=C_3=0.5\mu F\ R_o=200\Omega$	$V_{in}=48V\ L=2.4mH\ C=0.75\mu F\ R=200\Omega$
Fig. 9c	$V_{in}=12V\ L_1=L_2=0.6mH\ C_o=1\mu F\ R_o=200\Omega$	$V_{in}=18(21)V\ L=1.2mH\ C=1\mu F\ R=200\Omega$
Fig. 9d	$V_{in}=12V\ L_1=0.6mH$ $L_o=1mH\ C_1=C_2=0.5\mu F\ C_o=0.2\mu F\ R_o=200\Omega$	$V_{in}=18(21)V\ L=1.461mH$ $C=0.64\mu F\ R=200\Omega$

CONCLUSIONS

1. The optimization method of dynamic modes analysis are now widely used in the studies of mechanical systems and in quantum electrodynamics. Their use in electrical engineering remains scarce. At the same time, as is shown in this paper, they turn out to be exceptionally suitable and laconic means in analyzing the dynamics of DC-DC converters, making it possible, by applying simple tools, find the Euler-Lagrange equations for voltages and currents averaged values and the corresponding linear designs whose dynamics is identical to the dynamics of voltages and currents averaged values of in the converters under consideration.
2. Lagrange's energy function, the Lagrangian, is the most suitable in the studies of the dynamics of DC-DC converters, which makes it possible to study non-conservative systems.
3. This paper illustrates the use of optimization methods by the example of six base DC-DC converters. Along with that, we show the opportunities of its application on the example of four samples of enhanced converters with more complex designs including additional diodes and reactive components. Due to the analyzing of their Lagrangians, there arouses an opportunity to put in correspondence to them a conventional converter with the dynamics totally coinciding with that of the enhanced original converter.

REFERENCES

1. Middlebrook R. D., and Ćuk S. (1976), "A general Unified Approach to Modeling Switching-Converter Power Stages", IEEE PESC, 1976.
2. Tripathi A., Verma A. (2019), "Design and Implementation of Cuk Converter for Power Factor Correction of PMBLDC Motor Drive", Int. Journal of Recent Technology and Engineering (IJRTE), 8, (2S11), 2019; 2181-2193.

3. Vratislav M. V., Cottin D., Arno P. (2016), "Boost DC/DC converter nonlinearity and RHP-zero: Survey of the control-to-output transfer function linearization methods", Int. Conf. on Applied Electronics (AE), 2016; 10.
4. Hayes, B. (2016), "Nonlinear Dynamics of DC-DC Converters", A dissertation submitted in partial fulfillment of the requirements for the degree of Doctor of Philosophy at Dublin City University, School of Electronic Engineering, August 2016; 104 p.
5. Axelrod B., Beck Y., Berkovich Y. (2015), "High step-up DC-DC converter based on the switched-coupled-inductor boost converter and diode-capacitor multiplier: Steady state and dynamics", IET Power Electronics, 2015; 8(8): 1420-1428.
6. Axelrod B., Berkovich Y., Ioinovici A. (2005), "A new dynamic discrete model of DC-DC PWM converters", HAIT J. of Science and Engineering, B, 2(3-4), 2005; 1565-4990, 426-451.
7. Bahravar S., Mahery H. M., Babaei E., *et. al.* (2012), "Mathematical modeling and transient analysis of DC-DC buck-boost converter in CCM", Conf. Power Electronics (IICPE), IEEE 5th India Int. Conf., December, 2012.
8. Hsu S. P., Brown A., Rensink L., *et. al.* (1979), "Modeling and analysis of switching dc-to-dc converters in constant-frequency current programmed mode", Proc. IEEE Power Electron. Spec. Conf, 1979; 284–301.
9. Agrawal S., Verma M. Kr., Dwivedi P. K., *et. al.* (2014), "Modeling and Transient Performance Analysis of DC-DC Buck Converter", Vol. III, Issue V, IJLTEMAS**,** May 2014; 272-277.
10. Tse C. K. (2004), "Complex Behavior of Switching Power Converters", CRC Press, 2004.
11. Beck Y., Berkovich Y. (2020), "A Mathematical Model of Chaotic Processes in a Boost Converter: Generation and Synchronization", WJERT, 2020; 6(3): 435-459.
12. Beck Y., Berkovich Y. (2019), "Modes of Bifurcations, Chaos, and Undamped Oscillations in a Buck Converter with Feedback and Their Synchronizing", IJCEE, December 2019; 11(4): 164-174.
13. Zhioua M., Belghith S. (2014), "Analysis of the Chaotic Discrete Model of Boost Converter", Int. Conf. on Automation, Control, Engineering and Computer Science (ACECS'14), 2014; 5-11.
14. Gantmakher F.R. (2005), "Lectures on analytical Mechanics", Moscow, Fizmatlit Publ., 2005; 264.
15. Prigogine, I., Stengers, I. (1994), "The Time, Chaos and Quant", 1994.

16. Simonyi K., (1956), "Theoretische Elektrotechnik", VEB Deutscher Verlag der Wissenschaften, Berlin, 1956; 760.
17. Wells D. A. (1938), "Application of the Lagrangian Equations to Electrical Circuits", Journal of Applied Physics, 1938; 9(312). https://doi.org/10.1063/1.1710422.
18. Dennis J. B. (1959), "Mathematical Programming and Electrical Circuits", MIT and John Wiley & Sons, Inc., N-Y, 1959; 214.
19. Martyushev L.M., Seleznev V.D. (2006), "Maximum entropy production principle in physics, chemistry and biology", Physics Reports, 2006; 426: 1–45.
20. Landauer R. (1975)," Stability and entropy production in electrical circuits", J. Stat. Phys. 1975; 13: 1–16.
21. Axelrod B., Berkovich Y., Ioinovici A. (2005), "Transfer and Exchange of Power in DC-DC Converters in Similarity with Entropy Processes", Proceedings of Third IASTED Inter. Conf. Circuits, Signal and Systems, October 2005; 24-26.
22. Russer J., Russer P. (2012),"Lagrangian and Hamiltonian Formulations for Classical and Quantum Circuits", Electrical Engineering and Information Technology Department, Technische Universit¨at Munchen, 2012; 1-6.
23. Mayer, D. (2001), "Hamilton´s Principle and Electric Circuits Theory", Department of Theory of Electrical Engineering, Faculty of Electrical Engineering University of West Bohemia, Univerzitni 26, 30614 Pilsen, Czech Republic, 2001; 185-189.
24. Kadhim, Y. (2016), "Lagrangian description of electric circuits", Karlstad University, Faculty of Health, Science and Technology, Department of Engineering and Physics, January 22, 2016; 1-9.
25. Scherpen J., Klaassens J. B. Ballini L. (1999), "Lagrangian modeling and control of DC-to-DC converters", INTELEC'99, Copenhagen, 99CH37007, 1999; 31(14): 1-9.
26. Scherpen J., Jeltsema D., Klaassens J. B. (2003), "Lagrangian modeling of switching electrical networks", Systems & Control Letters, 2003; 48(5): 365–374.
27. Yildiz H. A., Goren-Sumer L. (2009), "Lagrangian Modeling of DC-DC Buck-Boost and Flyback Converters", European Conf. on Circuit Theory and Design, 2009; 245-248.
28. Sira-Ramirez H., Ortega R. and Escobar G. (1996), "Lagrangian Modeling of Switch Regulated DC-to-DC Power Converters", Proceedings of the 35th Conf. on Decision and Control Kobe, Japan, December 1996; 4492-4496.
29. Skandarnezhad A., Amangaldi Koochaki A., Mohammadmoradi Y., *et. al.* (2016), "Lagrangian Modelling of a Synchronous Step-Down Converter by Considering the Parasitic Elements", Przegląd Elektrotechniczny, ISSN 0033-2097, R, 2016; 92(3): 6-10.

30. Lee T.-S. (2004), "Lagrangian Modeling and Passivity-Based Control of Three-Phase AC/DC Voltage-Source Converters", IEEE Transactions on Industrial Electronics, August 2004; 51(4): 892-902.
31. Tan G., Chen H., Zhang X. (2008), "Comments on “Lagrangian Modeling and Passivity-Based Control of Three-Phase AC/DC Voltage-Source Converters”, IEEE Transactions on Industrial Electronics, April 2008; 55(4): 1881-1882.
32. Dworakowski P., Wilk A., Michna M., *et. al.* (2020), "Lagrangian model of an isolated dc-dc converter with a 3-phase medium frequency transformer accounting magnetic cross saturation", IEEE Transactions on Power Delivery, (Early Access), 2020; 1-10.
33. Noah M., Umetani K., Endo S., *et. al.* (2017), "A Lagrangian Dynamics Model of Integrated Transformer Incorporated in a Multi-phase LLC Resonant Converter", IEEE Energy 4onversion Congress and Exposition (ECCE), Oct. 2017; 1-5: 3781-3787.
34. Umetani, K. (2015), "Lagrangian Analysis Methodology for Power Electronics and Its Application to Industry", Interdisciplinary Graduate School of Science and Engineering, Shimane University, July 2015; 147.
35. White D. C., Woodson H. H. (1959), "Electromechanical Energy Conversion", New York, John Wiley and Sons, Inc,1959.
36. Soudakov V.F. (2014), "Hamiltonian Equations for Conservative Circuits with two Degrees of Freedom", Bauman MGTU, Moscow, Ser. "Instrument making", No1, 2014; 59-6.
37. Axelrod B., Berkovich Y., Moshe S. (2020), "Switched-Capacitor/Switched-Inductor Structures for Getting Transformerless Bidirectional DC–DC PWM Converters: Steady State and Dynamics", WJERT, 2020; 6(5): 435-459.